Design and Characterization of Dispersion Compensating Fiber Based on the LP_{01} Mode

A. Joseph Antos and David K. Smith

Abstract—**The practical implementation of erbium-doped fiber amplifiers with gain at 1.55 μm allows long unrepeatered transmission distances. However, in order to realize high data rates over these distances with already installed standard single mode fiber, techniques must be found to overcome the pulse spreading due to the positive chromatic dispersion of the transmission fiber in this window. We review a compensation technique based on propagating the signals through a specially designed fiber with large negative dispersion for the LP_{01} mode, thereby ending up with zero net pulse spreading. The basis of the concept are discussed and a key figure of merit for dispersion compensating devices is defined. The design and optimization of dispersion compensating (DC) fiber is described with special attention to practical concerns including packaging and manufacturability. We describe experimental fabrication results of DC fiber, results of using the fiber to make compact dispersion compensating modules, and the outcome of recent systems experiments incorporating the fiber.**

I. Introduction

THE practical implementation of erbium-doped fiber amplifiers (EDFA's) has reduced the importance of attenuation in the 1550 nm window as a key fiber-optic system design parameter. For example, errorless 5 Gb/s propagation has been demonstrated over 9000 km of dispersion-shifted fiber without the use of electronic regeneration [1]. However, the use of EDFA's to upgrade and simplify most existing fiber systems is presently limited by pulse dispersion since most installed fiber is nondispersion shifted which has low dispersion in the 1.3 μm window. The span length that is possible without electronic regeneration is limited by the pulse spreading that occurs with EDFA operation in the 1.55 μm window. For example, a length limit of about 100 km has been demonstrated for 5 Gb/s transmission over 1.3 μm-optimized fiber employing external modulation and direct detection techniques [2].

Several solutions to this problem have been suggested and can be categorized as either an active compensation technique that involves time-dependent manipulation of some aspect of the light pulse, or as a passive compensation technique which relies on time-independent properties of an optical element. Active solutions for digital transmission include prechirp techniques [3], [4] and a technique that uses the existing dispersion to convert a frequency modulated signal into an amplitude modulated signal at the receiver [5]. Passive techniques that have been demonstrated include the use of a fiber Gires–Tournois interferometric filter [6] and the use of the large negative waveguide dispersion of the LP_{11} mode of two-moded fiber [7]. Passive techniques that have been proposed include use of bulk gratings [8], gratings created in optical fiber used in reflection and transmission mode [9], [10], and wavelength-dependent coupling in multicore waveguide structures [11].

In this paper, we describe a passive technique which consists of including in the transmission path a length of fiber which has very large negative waveguide dispersion of the LP_{01} mode. The length of this fiber is chosen to obtain a negative pulse dispersion that is equal in magnitude to the positive dispersion accumulated by propagating through the transmission fiber. Earlier workers have examined the pulse equalization properties of short lengths of fiber of opposite dispersion to that of the transmission path [12], [13]. Here the compensating fiber is envisioned as possibly being quite long but deployed on a compact reel; the reel may be located at the transmission or receiver site or at any point along the transmission path. A standard transmission system would not tolerate the additional loss that results from propagating through the additional length of dispersion compensating (DC) fiber. In an amplified system, however, the additional loss is compensated by EDFA's that are present in the system. We first describe the basics of the concept and define a key figure of merit for this and other methods of dispersion compensation. We then describe our work to design and optimize the dispersion compensating (DC) fiber, in which one of the key constraints is the manufacturability of the fiber. A similar study of fiber optimization for large negative dispersion has recently been published [14]. In Section IV, we describe experimental results of fabrication of DC fiber, as well as results when the fiber was incorporated into compact dispersion compensating modules. In that section we also briefly describe systems experiments that have employed dispersion compensating modules. Finally we summarize the results.

II. Basic Principles

The total system pulse spreading per unit source bandwidth, $\Delta\tau$, due to propagation along a transmission path of standard single-mode fiber of length, l_s, and including a length of dispersion compensating fiber, l_c, is given by

$$\Delta\tau = D_s l_s + D_c l_c + D_s' l_s(\lambda - \lambda_1) + D_c' l_c(\lambda - \lambda_1) \quad (1)$$

where D_s and D_c are the first-order dispersion coefficients at wavelength λ_1 for standard and dispersion compensating fiber,

Manuscript received July 18, 1993; revised May 20, 1994.
The authors are with Corning Inc., Corning, NY 14831.
IEEE Log Number 9404388.

respectively, and D_s' and D_c' are the corresponding second-order dispersion coefficients, also known as the wavelength-dependent dispersion slopes. At 1550 nm, D_s and D_s' are typically 17 ps/nm-km and 0.07 ps/nm^2-km, respectively. When the signal wavelength is exactly λ_1, the system pulse spreading is zero if the length of the compensating fiber is given by

$$l_c = -\frac{D_c}{D_s} l_s. \tag{2}$$

For this length of fiber, the attenuation due to fiber loss is given by

$$\begin{aligned} L &= \alpha_s l_s + \alpha_c l_c \\ &= \left(\alpha_s + \alpha_c \frac{D_s}{|D_c|}\right) l_s \end{aligned} \tag{3}$$

where α_s and α_c are the standard fiber and compensating fiber loss per unit length. The second line of (3) leads us to define a figure of merit, M, that can be applied to the dispersion compensating fiber, namely, the amount of dispersion per unit loss

$$M = \frac{|D_c|}{\alpha_c} \tag{4}$$

with practical units of ps/nm-dB. While a large magnitude negative dispersion coefficient is desirable, it should not be obtained at the expense of greatly increased loss due to absorption, scattering, or macro- and micro-bending. Other passive dispersion compensating devices can be compared using this figure of merit.

One of the advantages of passive dispersion compensating methods is that the compensation requires no adjustment with change in source wavelength and should work equally well with multiwavelength narrow-band WDM systems. From (1), it may be seen that it is possible for a given transmission length l_s to obtain zero pulse spreading throughout a band of wavelengths by designing the compensating fiber so that it has a negative value for the dispersion slope, D_c'. It should be noted, however, that to obtain complete compensation through out a band, the magnitude of this negative slope must be greater than the magnitude of the slope of the standard fiber by the ratio of the transmission path length to the compensator length. Conversely, the negative impact of a positive dispersion slope of the compensating fiber is reduced by the ratio of lengths and the total dispersion slope is not significantly greater than that of dispersion-shifted fiber.

III. Dispersion Compensating Fiber Design

A. Computational Method

The model used to design Corning's dispersion compensating fiber is based on code that solves the scalar-wave equation for arbitrary index of refraction [15]. A schematic diagram of the relative index of refraction profile used is shown in Fig. 1, and is similar to designs used in standard dispersion-shifted fiber [16]. It consists of a parabolically shaped core region with peak relative index of Δ_p and a radius of r_c, a depressed cladding region with a depressed relative index with respect to pure silica of Δ_d and radius of r_d, and an index ring of relative index Δ_r and radius of r_r. This model simplifies for easy exploration of nonring profiles by setting both Δ_d and Δ_R equal to zero. In fact, given actual obtainable profiles, a parabolic profile more accurately describes obtainable simple profiles than the usual assumption of a rectangular step index. The wavelength dependence of the index of refraction is approximated using a six-term Sellmeier equation with coefficients found by a multiple regression fit to the germania-doped silica data of Kobayashi *et al.* [17]. For the wavelength dependence of refractive indexes of compositions with index lower than pure silica, this model assumes values that are extrapolations of the germania data.

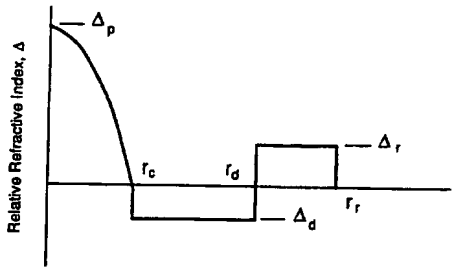

Fig. 1. Schematic model diagram of relative index of refraction profile showing parameters used in examining effect of index profile on dispersion characteristics.

For each index of refraction profile, the scalar-wave equation is solved for the LP_{01} field amplitude and propagation constant at seven wavelengths from 1475 to 1625 nm. Then the LP_{01} mode dispersion and its mode-field diameter are computed for wavelengths from 1525 to 1575 nm. The theoretical cutoff wavelengths for the LP_{02} and LP_{11} modes are found by searching for the maximum wavelengths that yield solutions to the scalar-wave equation when the propagation constant is at its minimum value, namely, that determined by the cladding index. The wavelength of the cutoff of the LP_{01} was used to determine a profile's susceptibility to macro-bend loss; it has been found empirically that a fiber is very bend sensitive at 1550 nm when its calculated LP_{01} cutoff wavelength is less than 1800 nm.

The profile solutions are iterated to an optimum using a Simplex algorithm [18]; the algorithm minimizes a weighted function of the differences between an iteration's calculated optical properties and the desired properties. The relative weights are adjusted to obtain practical and manufacturable profiles.

B. Model Results

To explore the range of possible negative dispersions, we plot the results of calculations for dispersion at a wavelength of 1550 nm in Figs. 2–4. Fig. 2 shows the range of negative dispersion that is possible with a simple parabolic profile as a function of core radius for five peak core relative indexes ranging from 1.5 to 2.5%. It is seen that for a given Δ_p,

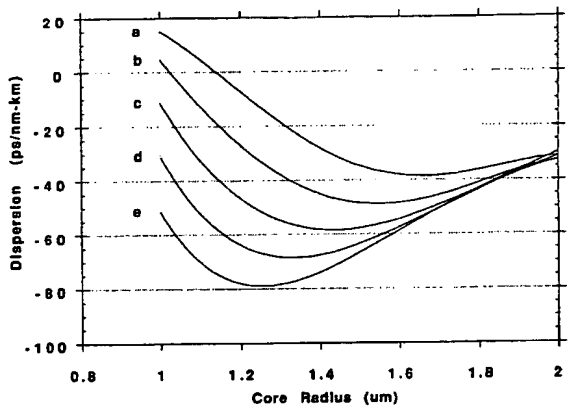

Fig. 2. Results of modeling showing dispersion as a function of core radius for an index profile without a depressed index region for different values of peak core relative index difference: (a) $\Delta_p = 1.5\%$, (b) $\Delta_p = 1.75\%$, (c) $\Delta_p = 2.0\%$, (d) $\Delta_p = 2.25\%$, and (e) $\Delta_p = 2.5\%$.

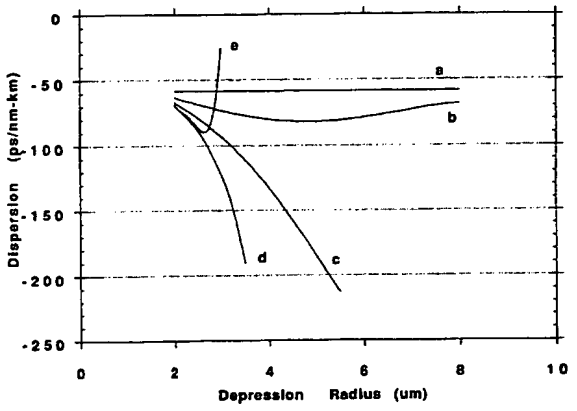

Fig. 3. Dispersion as a function of depressed region radius for the following depression relative indexes: (a) $\Delta_d = 0\%$, (b) $\Delta_d = 0.1\%$, (c) $\Delta_d = 0.2\%$, (d) $\Delta_d = 0.3\%$, and (e) $\Delta_d = 0.4\%$. The core relative index and radius are held constant at 2% and 1.4 μm, respectively.

a maximum negative dispersion occurs at an optimum core radius in the range from 1 to 2 μm, and that the value of the maximum negative dispersion as well as the optimum core radius decrease with increasing Δ_p. Addition of a depressed index region outside of the core greatly increases the value of a fiber's negative dispersion. Fig. 3 shows the impact of depth and width of a depressed region (with no increased index outer ring) for a fixed peak core index of 2% and core radius of 1.4 μm. Within a region of index depression from 0% to about 0.35%, the negative dispersion increases to nearly -200 ps/nm-km as the depression radius is varied in the range of 3–6 μm. When the depression index is 0.4% or greater, however, the index only increases slightly before decreasing to values less than even the simple parabolic solution. Even larger magnitudes of negative dispersion are possible if one further optimizes the core for a given depression index. An example is shown in Fig. 4, where the impact of core radius on dispersion is seen with a peak core index of 2% and a fixed depression radius of 4.5 μm. Values of negative dispersion greater than -300 ps/nm-km are theoretically obtainable.

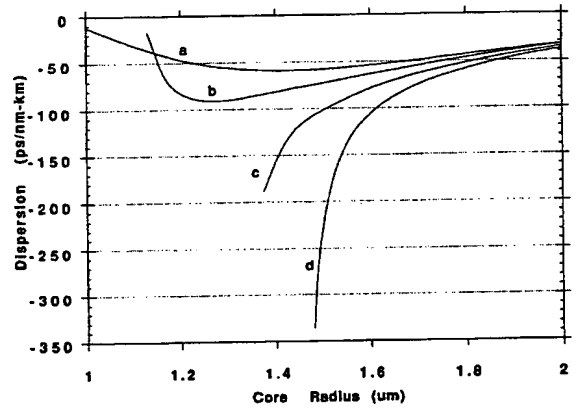

Fig. 4. Dispersion as a function of core radius for a dispersion compensating fiber design with radius of the depressed region of 4.5 μm for the following depressed region indexes: (a) $\Delta_d = 0\%$, (b) $\Delta_d = 0.1\%$, (c) $\Delta_d = 0.2\%$, and (d) $\Delta_d = 0.3\%$.

Designs with the model index profile have a waveguide component of the total dispersion that decreases from the value at short wavelengths to a minimum occurring in the range of 1.4–1.6 μm. One of the main impacts of inclusion of a depressed index region and an outer ring is to increase the difference between waveguide dispersion at short wavelengths and the minimum value. It also shifts the wavelength at which the minimum waveguide dispersion occurs toward longer wavelengths. The net impact is to obtain a design with a negative dispersion slope versus wavelength curve through the operating wavelength band. The total dispersion thus obtained can have a negative dispersion slope that can offset some of the positive dispersion slope of standard transmission fiber. The magnitude of the negative slopes that are calculated is less than the positive slopes of standard fiber; thus, given the length impact of the transmission fiber and compensating fiber, the total dispersion slope of the band is not greatly affected.

Because of the impact of attenuation on a compensator's figure of merit, M, it is prudent to use the model to examine the impact of design on loss before attempting to fabricate fibers from one of these designs. Potential sources for loss greater than the typical loss of 0.25 dB/km for dispersion shifted fiber are increased absorption and scattering from higher levels of index-raising dopants, loss from bend sensitivity, and loss from stress imbalance between the core and cladding that results from large thermal expansion differences. While increase in loss due to absorption and scattering in fibers with high levels of germania in the light guiding region is well known [19], loss due to this effect is expected to increase by only 0.1–0.2

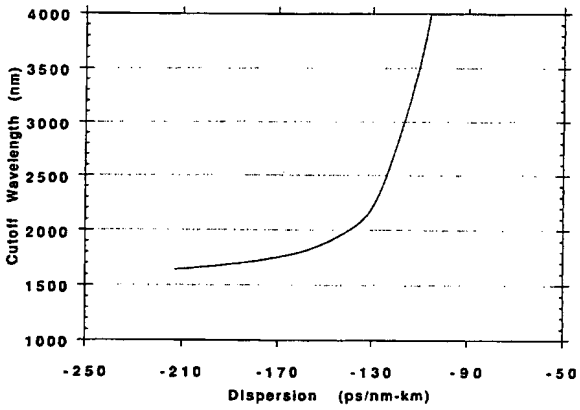

Fig. 5. Cutoff wavelength of the fundamental LP_{01} mode as a function of the dispersion at $\lambda = 1550$ nm for a peak core relative index of 2%, core radius of 1.4 μm, and depressed region index of 0.2%.

dB/km. Of much greater concern are macro-bending losses that occur from coiling the dispersion compensating fiber onto a practical-size reel, and micro-bending losses that may manifest themselves during temperature excursions of the fiber in its operating environment. Unlike the solutions for a step-index profile, profiles that include a depressed index region outside the core have a finite cutoff wavelength for the propagation of the LP_{01} mode. One indicator of the susceptibility of a design to bending loss is the wavelength at which this mode is no longer a propagating solution to the wave equation (i.e., the wavelength at which the LP_{01} mode is cut off); to be stable against macro- and micro-bending, one requires that the LP_{01} cutoff wavelength be large relative to the operating wavelength. Some of this information is implicitly contained in Figs. 3 and 4; data points that have the most negative dispersion values have an LP_{01} cutoff wavelength at 1625 nm, i.e., only 50–60 nm from the EDFA operating band. Thus, these solutions are expected to be very bend sensitive. To explore this further, Fig. 5 shows a plot of LP_{01} cutoff wavelength as a function of dispersion where the varying dispersion was obtained by varying the depression radius, r_d, for a design with $\Delta_p = 2.0\%$, $r_c = 1.4$ μm, and $\Delta_d = 0.2\%$. We find that the LP_{01} cutoff wavelength does not become large relative to the operating wavelength until we get into designs with a modest negative dispersion at and above -130 ps/nm-km.

The model can be used to indicate ease of manufacture by performing studies to determine if a design is insensitive to changes in geometry and index. Manufacturing considerations also drive designs from attempting to optimize solely on large negative dispersion. For example, one decision was to limit Δ_p to values of 2% or less, since higher values result in the cracking of forms due to large thermal expansion differences.

While modeling is absolutely necessary for dispersion fiber optimization, uncertainties in loss mechanisms and manufacturing tolerance capabilities compel the actual fabrication of a variety of profiles to verify the directions suggested by modeling.

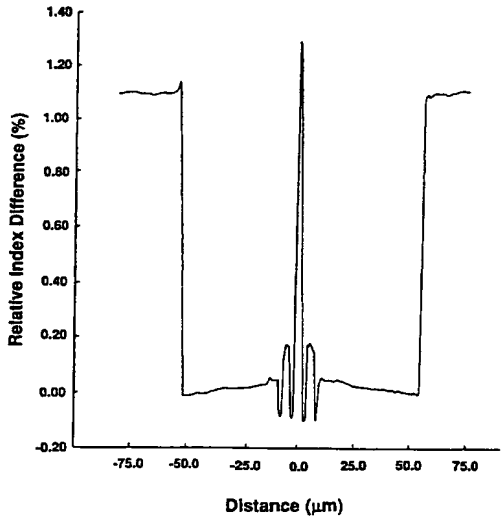

Fig. 6. Refractive near-field (RNF) measurement of the relative index of refraction profile of a dispersion compensating design of Type D that yielded -100 ps/nm-km dispersion at 1550 nm.

IV. Experimental Results

A. Fiber Results

Fibers were fabricated using the outside vapor deposition technique [20] with germania used as an index-increasing dopant and fluorine used as an index-decreasing dopant. Fig. 6 shows an example of the refractive index profile of the fiber labeled Type D below; it has a segmented core and an index depressed region and a ring. Using a range of profiles, we have experimentally obtained dispersion ranging from -45 to -100 ps/nm-km, attenuation from 0.4 to 1.2 dB/km, and range of figure of merit from between 50 and 160 ps/nm-dB at $\lambda = 1550$ nm. Fig. 7(a) and (b) shows examples of dispersion and attenuation variation with wavelength for Type B and Type D fibers.

Experimental results of dispersion, dispersion slope, attenuation, and figure of merit, all at $\lambda = 1550$ nm, for four fibers with distinct index profiles are listed in Table I. Fiber profile Type A is a step-index design, while B, C, and D are segmented core designs with an index depressed region with different core and ring diameters.

B. Packaged DC Fiber Results

We have designed a compact reel with a hub radius of 7.6 cm, height of 4.3 cm, and a flange diameter of 16.5 cm. A 200 μm acrylate coating makes this reel capable of holding sufficient dispersion compensating fiber to correct for up to 1360 ps/nm dispersion. This amount of dispersion can typically be accumulated from propagating through 80 km of standard single mode fiber. No increase in attenuation was observed as a result of the 7.6 cm minimum radius bend. Micro-bending effects were investigated by monitoring loss changes during temperature cycling of the assembly. An increase in loss of ≤ 0.6 dB relative to the room-temperature value is typically

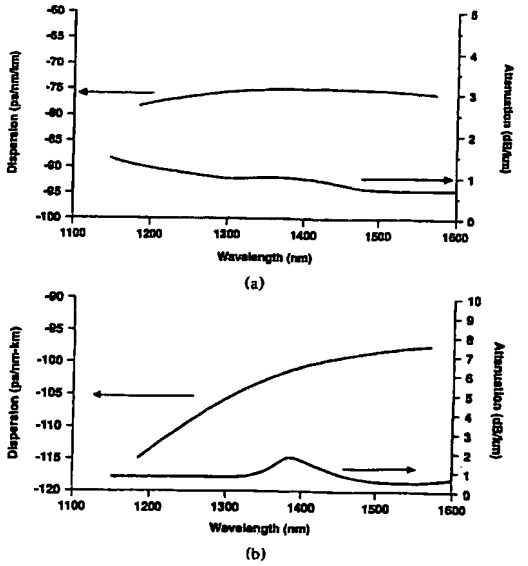

Fig. 7. Dispersion and attenuation as a function of wavelength for dispersion compensating fiber of profile (a) Type B and (b) Type D.

TABLE I
EXPERIMENTAL VALUES OF PARAMETERS OF FOUR DIFFERENT PROFILES OF DISPERSION COMPENSATING FIBER DESCRIBED IN THE TEXT. ALL VALUES MEASURED AT $\lambda = 1550$ NM

Fiber Profile Type	Total Dispersion, D_C (ps/nm-km)	Dispersion Slope, D'_C (ps/nm^2-km)	Attenuation, α (dB/km)	Figure of Merit, M (ps/nm-dB)
A	-45	0.07	0.40	75
B	-90	0.00	0.65	140
C	-77	-0.02	0.60	130
D	-100	0.07	0.65	155

observed within a temperature range from -40 to $+85$°C, while a loss increase of ≤ 0.2 dB is observed in the limited range from 0 to $+65$°C.

Another important issue with a practical dispersion compensating device is the splice loss that arises from connecting DC fiber to standard single mode fiber. Mode field diameters of the various designs fabricated range from 4 to 6 μm, while standard matched clad fiber typically has a mode field diameter of 10.5 ± 1.0 μm at 1550 nm. Calculations of intrinsic splice loss as a result of mode field mismatch predict that the splice loss should range from 1 to 3 dB. Actual values of splice loss obtained by optimizing fusion splicer parameters and using long electric arc times are considerably below the calculated value with a typical splice loss of 0.5 ± 0.1 dB.

C. System Tests

System tests incorporating DC fibers and EDFA's have been performed. Fig. 8 shows the optical schematic of a test

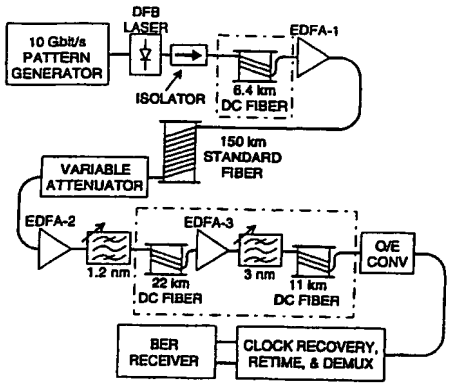

Fig. 8. Optical schematic diagram of a system measurement designed to test the transmission of 10 Gb/s signals over 150 km of standard single-mode fiber using a drive-current modulated DFB laser and direct detection.

performed in conjunction with workers at Alcatel Network Systems [21] to evaluate the feasibility of transmitting 10 Gb/s directly modulated, direct-detection signals over 150 km of standard fiber. The DC fiber used in the test had a dispersion of -65 ps/nm-km at $\lambda = 1550$ nm, an attenuation of 0.48 dB/km, and a compensator figure of merit of 135. The wavelength variation of the dispersion of the fiber over the region from 1525 to 1575 nm was small with a dispersion slope of about 0.008 ps/nm^2-km. The 150 km of transmission fiber required about 39 km of DC fiber to correct for the dispersion. The DC fiber added an insertion loss of about 19 dB. Three single-pumped 980 nm amplifiers were used to make up for the 33 dB transmission link loss and the additional loss of the compensating fiber. The DC fiber was placed in three locations. The first reel (6.4 km), representing about 3 dB loss, was located before the power amplifier, taking advantage of the fact that the amplifier's saturated output power of 11 dBm could be reached by less input power than was available from the signal source. Two amplifiers at the receiver end of the link acted as both a compensator and a two-stage preamplifier. The receiver amplifiers were followed by reels of 22 km (10.6 dB insertion loss) and 11 km (5.3 dB insertion loss) of DC fiber, respectively. The amplifiers were operated at gains of 25 and 31 dB, respectively, and both were followed by narrow-band dielectric filters to reduce the impact of ASE buildup and spontaneous-spontaneous beat noise at the receiver. Fig. 9 shows the results of bit-error rate measurements made using multiplexed 5 Gb/s pseudorandom bit streams and a $2^{31} - 1$ pattern over 150 km of transmission fiber. A receiver power penalty of less than 1 dB was seen as a result of the transmission that may be the result of nonoptimization of the EDFA preamp.

A test of another application requiring dispersion compensation was performed in conjunction with Bellcore [22]. Here, dispersion compensating fiber was used to allow simultaneous 1310 and 1550 nm directly modulated, direct-detection SONET transmission at 2.5 Gb/s over 60 km of standard fiber (Fig. 10). The 1310 nm signal was demultiplexed from the transmission fiber using a WDM that added about 0.55 dB

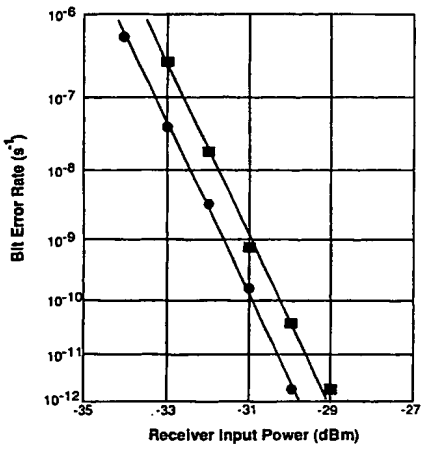

Fig. 9. Bit-error rate diagrams showing results of back-to-back and transmission through 150 km of standard fiber for the experiment shown in Fig. 8.

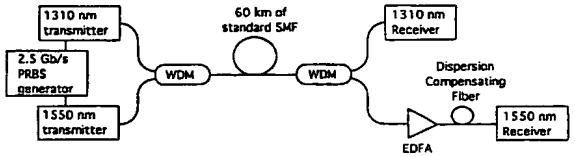

Fig. 10. Optical schematic diagram of a system test to evaluate the simultaneous transmission of 1.3 and 1.55 μm signals over the same fiber of length 60 km.

to that leg so that it could be detected without amplification. The total gain of the EDFA was 19 dB, which more than compensated for the 16 dB loss of the compensator fiber. No power penalty was observed in the 1310 or 1550 nm legs as a result of propagation through the transmission fiber when compared to back-to-back results.

V. Conclusions

While use of EDFA's and dispersion-shifted transmission fiber optimized for operation at 1.55 μm is an obvious choice for future long-haul telecommunication systems, amplifiers with dispersion compensation based on LP_{01} mode propagation can enable currently installed standard single-mode fiber systems to reap the benefits of EDFA's. Compact reels holding specially designed fiber provide a stable and robust method that works well with both single-frequency and wavelength-division multiplexed systems. Further work is required to optimize the balance of dispersion and loss characteristics as measured by the compensator fiber figure of merit. Also, further system experimentation is also required to find the true limitations of this method.

Acknowledgment

We thank M. Dugan, A. J. Price, C. Lin, and H. Izadpanah for their measurements and direction regarding applications and systems requirements. It is a pleasure to acknowledge the contributions of our co-workers at Corning: E. F. Murphy, D. W. Hall, R. Knowlton, T. Webb, and J. Grissom.

References

[1] N. S. Bergano, C. R. Davidson, G. M. Homsey, D. J. Kalmus, P. R. Trischitta, J. Aspell, D. A. Gray, R. L. Maybach, S. Yamamoto, H. Taga, N. Edagawa, Y. Yohida, Y. Horiuchi, T. Kawazawa, Y. Namihira, and S. Akiba, "9000 km, 5 Gb/s NRZ transmission experiment using 274 erbium-doped fiber-amplifiers," in *Opt. Amplif. Appl. Tech. Dig.*, vol. 17, Opt. Soc. Amer., Washington, DC, 1992, Postdeadline Paper 11.

[2] M. Suzuki, H. Tanaka, H. Taga, S. Yamamoto, and Y. Matsushima, "$\lambda/4$ shifted DFB laser/electroabsorption modulator integrated light source for multigigabit transmission," *J. Lightwave Technol.*, vol. 10, pp. 90–94, 1992.

[3] A. H. Gnauck, L. J. Cimini, J. Stone, and L. W. Schultz, "Optical equalization of fiber chromatic dispersion in a 5 Gb/s transmission system," *IEEE Photon. Technol. Lett.*, vol. 2, pp. 585–587, 1990.

[4] N. Hemni, T. Saito, M. Yamaguchi, and S. Fujita, "10 Gb/s, 100 km normal fiber transmission experiment employing a modified prechirp technique," in *Opt. Fiber Commun. Conf. 1991 Tech. Dig. Series*, vol. 4, Opt . Soc. Amer., Washington, DC, 1991, p. 54.

[5] B. Wedding, "New method for optical transmission beyond the dispersion limit," *Electron. Lett.*, vol. 28, pp. 1298–1300, 1992.

[6] A. H. Gnauck, C. R. Giles, L. J. Cimini, Jr., J. Stone, L. W. Stulz, S. K. Korotky, and J. J. Veselka, "8-Gb/s-130 km transmission experiment using Er-doped fiber pre-amplifier and optical dispersion equalization," *IEEE Photon. Technol. Lett.*, vol. 3, pp. 1147–1149, 1991.

[7] C. D. Poole, J. M. Wiesenfeld, A. R. McCormick, and K. T. Nelson, "Broadband dispersion compensation by using the higher-order spatial mode in a two-mode fiber," *Opt. Lett.*, vol. 17, pp. 985–987, 1992.

[8] O. E. Martinez, *IEEE J. Quantum Electron.*, vol. QE-23, pp. 59–64, 1987.

[9] F. Ouellette, "All-fiber filter for efficient dispersion compensation," *Opt. Lett.*, vol. 16, pp. 303–305, 1991.

[10] ——, "Dispersion cancellation using linearly chirped Bragg grating filters in optical waveguides," *Opt. Lett.*, vol. 12, pp. 847–849, 1987.

[11] F. Ouellette and Y. Duval, "Optical equalization with linearly tapered two-dissimilar-core fiber," *Electron. Lett.*, vol. 27, pp. 1668–1669, 1991.

[12] C. Lin, H. Kogelnik, and L. G. Cohen, "Optical-pulse equalization of low-dispersion transmission in single-mode fibers in the 1.3–1.7 mm spectral region," *Opt. Lett.*, vol. 5, pp. 476–478, 1980.

[13] D. S. Larner and V. A. Bhagavatula, "Dispersion reduction in single-mode-fiber links," *Electron. Lett.*, vol. 21, pp. 1171–1172, 1985.

[14] A. M. Vengsarkar and W. A. Reed, "Dispersion-compensating single-mode fibers: Efficient designs for first- and second-order compensation," *Opt. Lett.*, vol. 18, pp. 924–926, 1993.

[15] D. Gloge, "Weakly guiding fibers," *Appl. Opt.*, vol. 10, pp. 2252–2258, 1971.

[16] V. A. Bhagavatula, M. S. Spotz, and W. F. Love, "Dispersion-shifted segmented-core-single-mode fibers," *Opt. Lett.*, vol. 19, pp. 186–188, 1984.

[17] S. Kobayashi, S. Shibata, N. Shibata, and T. Izawa, "Refractive index dispersion of doped fused silica," in *Proc. IOOC'77*, 1977, pp. 309–312, Paper B8-3.

[18] J. A. Nelder and R. Mead, "A simplex method for function minimization," *Computer J.*, vol. 7, pp. 308–313, 1965.

[19] N. Shibata, M. Kawachi, and T. Edahira, "Optical loss characteristics of high-GeO_2 content silica fibers," *Trans. IECE* (Japan), vol. E65, p. 12, 1980.

[20] M. G. Blankenship and C. W. Deneka, "The outside vapor deposition method of fabricating optical waveguide fiber," *J. Quantum Electron.*, vol. QE-18, pp. 1418–1423, 1985.

[21] J. M. Dugan, A. J. Price, M. Ranadan, D. L. Wolf, E. F. Murphy, A. J. Antos, D. K. Smith, and D. W. Hall, "All-optical, fiber-based 1550 nm dispersion compensation in a 10 Gb/s, 150 km transmission experiment over 1310 nm optimized fiber," in *Opt. Fiber Commun.*, vol. 5, *1992 OSA Tech. Dig. Series*, Opt. Soc. Amer., Washington, DC, 1992, Paper PD-14.

[22] H. Izadpanah, C. Lin, J. L. Gimlett, A. J. Antos, D. W. Hall, and D. S. Smith, "Dispersion compensation in 1310 nm-optimized SMFs using optical equalizer fiber, EDFAs and 1310/1550 nm WDM," *Electron. Lett.*, vol. 28, pp. 1469–1470, 1992.

A. Joseph Antos received the B.S. degree in chemical engineering from Lehigh University in 1981 and the M.S. degree in chemical engineering practice from the Massachusetts Institute of Technology in 1982.

In 1983 he joined Corning Incorporated as a Development Engineer at the Wilmington Plant. In 1991 he joined the Telecommunication Product Development group at Corning's Sullivan Park Laboratory. He became Supervisor of the Fiber Development group in August 1993. He holds 4 patents in the field of optical fiber fabrication.

David K. Smith received the B.S. and M.S. degrees in chemical engineering from the University of Michigan, and the M.S. degree in statistics from Rutgers University.

He worked in R&D for Dupont from 1961 to 1973. He has been with R&D, Corning Inc., since 1973. He specializes in mathematical modeling and statistical analysis.

Mr. Smith is a member of ASA.